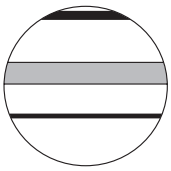

Research paper

The Holocene
21(2) 327–341

DOI: 10.1177/0959683610374882
http://hol.sagepub.com
SAGE

Linking tree-ring and sediment-charcoal records to reconstruct fire occurrence and area burned in subalpine forests of Yellowstone National Park, USA

Philip E. Higuera, Cathy Whitlock and Josh A. Gage[1]
Montana State University, USA

Abstract

Reconstructing specific fire-history metrics with charcoal records has been difficult, in part because calibration data sets are rare. We calibrated charcoal accumulation in sediments from three medium (14–19 ha) and one large (4250 ha) lake with a 300 yr tree-ring-based fire-history reconstruction from central Yellowstone National Park (YNP) to reconstruct local fire occurrence and area burned within a 128 840 ha study area. Charcoal peaks most accurately reflected fires within 1.2–3.0 km of coring sites, whereas total charcoal accumulation correlated best with area burned within 6.0–51 km (r^2=0.22–0.62, p<0.05). To reconstruct area burned for the entire study area, we developed a statistical model based on a composite charcoal record. The model explained 64–79% of the variability in area burned from AD 1675 to 1960 and was robust to cross-validation. Reconstructed area burned from AD 1240–1975 was significantly higher during periods including extreme annual drought (p=0.05), and area burned varied significantly at ≈ 60 yr timescales (p<0.05), similar to the variability in an independent precipitation reconstruction covering the same period. Widespread burning (>10 000 ha) occurred at 150–300 yr intervals, and at the site level, fire probability increased with stand age (composite Weibull c parameter = 1.61 [95% CI 1.36–2.54]), both suggesting that post-fire stand development played an important intermediary role between climate and fire by increasing fuel abundance and probability of fire spread. Our study illustrates the possibility of reconstructing area burned with multiple charcoal records, and results imply that future fire regimes in YNP will be governed by direct impacts of altered moisture regimes and by vegetation dynamics affecting the abundance and continuity of fuels.

Keywords

calibration, charcoal analysis, climate change, fire history, *Pinus contorta*, wildfires

Introduction

Fire is a dominant natural disturbance in forested ecosystems linking climate change and biosphere response. Understanding these linkages has become an important priority, particularly in western North America, where numerous large stand-replacing fires have occurred in recent years (e.g. National Interagency Fire Center, 2008: http://www.nifc.gov/fire_info/fire_stats.htm). Fire-history reconstructions from tree-ring and lake-sediment records are the primary source of information for evaluating the precedence of current and future fire activity (Conedera *et al*., 2009). Tree-ring records provide fire-history information with high temporal resolution for the last 300–500 yr, whereas high-resolution charcoal records are more widely spaced geographically, offer decadal- to multidecadal-scale resolution, and span millennia.

Testing the assumptions of charcoal-based fire history studies is a critical goal for paleofire research. In the western USA, this work began in Yellowstone National Park (YNP), where Whitlock and Millspaugh (1996) collected sediment samples in small lakes in burned and unburned watersheds to understand post-fire charcoal accumulation. Millspaugh and Whitlock (1995) used these insights to develop a 750-yr-long fire history based on sediment charcoal from five lakes in central YNP, comparing the age of charcoal peaks with a regional fire chronology based on tree-ring data (Romme and Despain, 1989). These initial studies did not quantify the spatial domain represented by charcoal peaks, nor did they interpret overall charcoal abundance.

Since the early work in YNP, our understanding of sediment-charcoal records and the techniques used to infer fire history have greatly improved. For example, statistical analyses have allowed reconstructions of fire history at small spatial scales by decomposing charcoal time series into 'background' and 'peak' components, and applying a threshold based on (semi-) objective criteria to identify samples likely associated with local fire events (e.g. Clark *et al*., 1996; Gavin *et al*., 2006; Higuera *et al*., 2009; Long *et al*., 1998). Support for these techniques comes from empirical studies linking known fires with charcoal accumulation (Gardner and Whitlock, 2001; Gavin *et al*., 2003; Higuera *et al*., 2005; Lynch *et al*., 2004; Tinner *et al*., 1998) and process-based models that consider charcoal production, dispersal, and deposition

Received 2 October 2009; revised manuscript accepted 26 April 2010
[1]Present address: American Wildlands, P.O. Box 6669, Bozeman MT 59715, USA

Corresponding author:
Philip E. Higuera, Department of Forest Ecology and Biogeosciences, Box 441133, University of Idaho, Moscow ID 83844, USA
Email: phiguera@uidaho.edu

(Clark, 1988b; Higuera *et al*., 2007; Peters and Higuera, 2007). CharSim (Higuera *et al*., 2007) is a recently developed process-based model that incorporates fire history, primary and secondary charcoal transport, sediment mixing, and sediment sampling to create sediment-charcoal records based on a user-defined fire regime. In addition to supporting the assumption that charcoal peaks reflect fire occurrence at small spatial scales (*c*. 1 km radius), a major prediction from CharSim is that overall trends in macroscopic charcoal reflect area burned at larger spatial scales (*c*. 10+ km radius). Although this prediction is valuable for the interpretation of charcoal records (e.g. Brubaker *et al*., 2009; Marlon *et al*., 2008, 2009), it has received little direct or indirect empirical testing (but see Duffin *et al*., 2008).

The original YNP data set analyzed by Millspaugh and Whitlock (1995) remains one of the most complete calibration data sets for testing this and other key questions about the nature of sediment-charcoal records. In this study, we revisit these data and apply new techniques for their comparison and interpretation. Specifically, spatially explicit comparisons between charcoal and tree-ring records help to (1) statistically calibrate charcoal records to detect both 'local' fire occurrence and 'extra local' area burned and (2) test the theoretical relationships between area burned and charcoal accumulation inferred from CharSim. We then develop a composite record of fire occurrence and a statistical model reconstructing area burned from AD 1225 to 1975. This exercise serves as a case study to demonstrate the potential for reconstructing fire occurrence and area burned at well-defined spatial scales, where both charcoal and tree-ring data sets are available. The value of this approach is illustrated by a comparison of the area-burned reconstruction to a precipitation reconstruction for the YNP region (Gray *et al*., 2007). Our objectives were to answer the following questions: (1) What metrics of fire regimes (e.g. fire occurrence, fire size, area burned) are recorded by charcoal data and at what spatial scales? (2) How can combining charcoal records yield information on regional fire history, and in particular area burned? And (3) how do changes in regional fire history compare with variations in precipitation over the last 750 yr in central YNP?

Methods and rationale

Study area and stand-age reconstruction

Four sites were used in this study (Figure 1). Duck (44°25'N, 110°35'W, elev. 2374 m, 14.2 ha, water depth 18.5 m), Mallard (44°28'N, 110°47'W, elev. 2454 m, 13.7 ha, water depth 9.1 m), and Dryad (44°33'N, 110°31'W, elev. 2530 m, 18.5 ha, water depth 8.5 m) lakes are fed by small inlet streams and have no outlet streams. West Thumb (44°26'N, 110°32'W, elev. 2357 m, 4250 ha, water depth 81 m) is a large sub-basin of Yellowstone Lake. The Central Plateau of YNP is dominated by infertile substrates from rhyolite volcanic rocks, which support lodgepole pine (*Pinus contorta* Dougl. var. *latifolia*) in about 80% of the forested area (Despain, 1990). The combination of homogenous vegetation and subdued topography should minimize the impact that these variables have on charcoal dispersal and deposition. In combination with a historic regime of large, infrequent, stand-replacing fires (Romme and Despain, 1989), these attributes make the Central Plateau an ideal location for linking tree-ring and sediment-charcoal records and comparing results to CharSim.

A tree-ring-based stand-age map developed by Romme and Despain (1989) and published by Tinker *et al*. (2003) was used to estimate area burned from AD 1675 to 1975 (Figure 1). The coverage was obtained from DB Tinker as an Arc/Info shapefile and converted to raster format with a cell size of 100 m using ArcGIS (ESRI Inc., Redlands CA). Stand ages within the 128 840 ha study area were estimated from 5–10 increment cores from the dominant lodgepole pine in forest patches > 4 ha. We summarized this reconstruction considering two important sources of error. First, stand ages provide a minimum time-since-fire, because post-fire lodgepole pine regeneration occurs over several years, and tree cores taken above the root crown underestimate tree age (Agee, 1993). We thus binned stand ages in 15-yr intervals. Second, more recent fires erase evidence of older fires, and area burned by older fires is likely underestimated. We accounted for this fading record by using AD 1675 as the oldest stand age in our analysis, even though the data set includes trees dating to AD 1425 (Romme and Despain, 1989; Tinker *et al*., 2003; Figure 1).

Sediment records

Sediment-charcoal data collected by Millspaugh and Whitlock (1995) were analyzed with newly developed methods to estimate fire history over the past 500–750 yr. Briefly, charcoal particles 125–250 μm in diameter were quantified from 5 cm^3 samples taken from continuous 1 cm intervals. Chronologies for the last 150–200 yr were based on ^{210}Pb methods using the constant rate of supply model (Appleby and Oldfield, 1978); the age of older sediments was estimated using the cumulative dry weight of the interval and the mean sediment accumulation rate for the dated portion of the cores (Whitlock and Millspaugh, 1996). The original age extrapolation was justified given similarity between estimated sedimentation rates over the past several centuries and those in better-dated sites in YNP (Huerta *et al*., 2009; Millspaugh *et al*., 2000). Sediment accumulation rates were used to calculate charcoal accumulation rates (CHAR, pieces/cm^2 per yr) and resulted in median sample resolutions of 8, 10, 7, and 13 yr/sample at Duck, Mallard, Dryad, and West Thumb, respectively. Prior to analysis, all records were interpolated to 15 yr intervals to account for varying sampling resolution within and between sites and for comparisons with the tree-ring record.

Calibrating charcoal records to detect fire occurrence and defining 'local' spatial scales

To identify charcoal peaks potentially related to 'local' fire occurrence, we decomposed each charcoal series by subtracting 450 yr trends (aka 'background' charcoal; estimated with a locally weighted regression robust to outliers) to obtain a 'peak' CHAR series. We used a Gaussian mixture model to define noise-related variations in the entire peak series (Gavin *et al*., 2006) using the program CharAnalysis (Higuera *et al*., 2009; available online at http://code.google.com/p/charanalysis/). For each record, we considered three possible global threshold values ('peak thresholds') for separating noise-related from fire-related variations in peak CHAR, defined by the 95th, 99th, and 99.9th percentiles of the noise-related Gaussian distribution.

We evaluated the accuracy of peak-inferred fires by comparing identified peaks with tree-ring-inferred fires ('true fires'; Appendix 1, Figure A1). Accuracy was defined as the true-positive rate (proportion of peaks correctly identifying fires) minus the false-positive rate (proportion of peaks incorrectly identifying fires). For example, consider a record that has a total of four charcoal peaks; three of these peaks match three true fires, while one

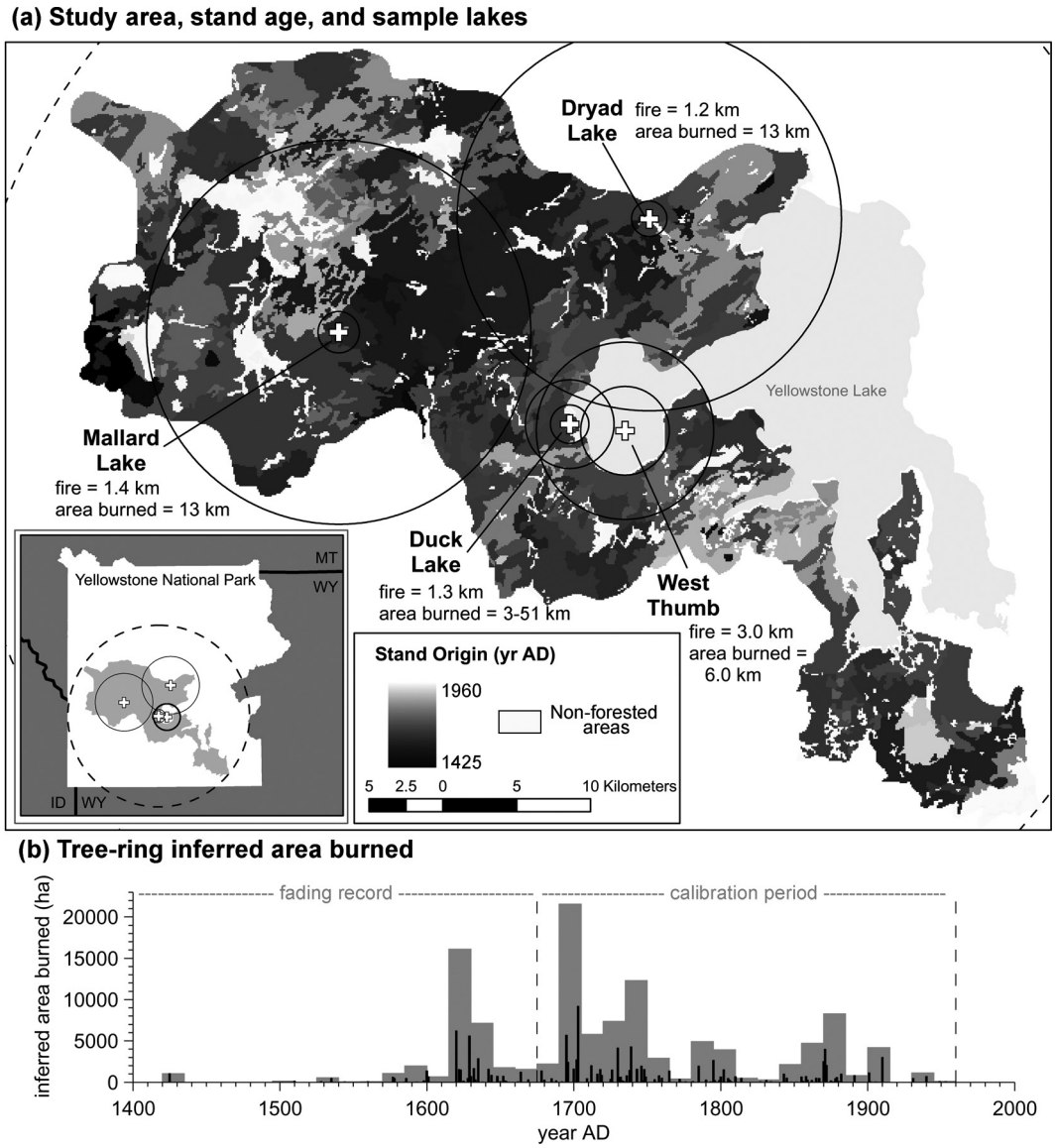

Figure 1. Study area, sample lakes, and tree-ring-based area burned record. (a) The location of each study lake within the Tinker *et al.* (2003) study area on the Yellowstone Plateau and Yellowstone National Park (inset). Smaller circles around each lake identify the optimal spatial scale for comparing identified peaks to tree-ring-inferred fire events ('fire'), and larger circles identify the optimal spatial scale for correlating charcoal accumulation rates to tree-ring-inferred area burned ('area burned'). Note that the larger dashed circle around Duck Lake encompasses the entire study area and is largely an estimate. Stand-age patches are based on the data set of Romme and Despain (1989) and Tinker *et al.* (2003). (b) Time series of area burned, inferred from the stand-age map in (a), at annual (black) and 15 yr (gray) intervals. Similar to Romme and Despain (1989), we assume that stand age before AD 1675 represents an unknown fraction of total area burned ('fading record')

charcoal peak does not match a true fire. The accuracy for this scenario would be ⅗ (true positive rate) − ¼ (false positive rate) = 0.75. True fires were defined as those falling within 30 yr (two time steps) of an inferred fire (i.e. charcoal peak), and any area burned within a 15 yr time step was classified as a fire, regardless of the number or spatial pattern of cells contributing to the area burned. We used accuracy to identify (1) the optimal of the three peak threshold criteria considered, and (2) the 'optimal spatial scale', the radius at which charcoal peaks best represent true fires (Higuera *et al*., 2007). The optimal spatial scale was determined by calculating accuracy when comparing inferred and true fires within concentric circles with radii of 0.1 to 10 km, centered on the coring site (Figure 1). Using total area burned as a proxy for fire size, we also tested if accuracy varied with fire size by calculating accuracy based on true fires defined as 15 yr periods with >10 and >100 ha burned.

Correlating charcoal accumulation and area burned and defining 'extra local' spatial scales

We compared total CHAR to area burned within varying distances of each sediment core (0.1–43 km) to determine if CHAR-area burned correlations were statistically significant (Appendix 1, Figure A2). This approach mirrors Higuera *et al*. (2007), in which simulated charcoal records were compared with fire histories using CharSim. We expected that (1) charcoal deposition would correlate with area burned at multiple distances, and (2) correlations would increase as more area was included in the comparison, reaching a maximum around 10 km, and decreasing at greater distances. We allowed for errors related to chronologies and taphonomy (e.g. charcoal deposition lagging fire occurrence and sediment mixing; Duffin *et al*., 2008; Whitlock and Millspaugh, 1996) by correlating area burned with CHAR series lagged −30, −15, 0, 15,

30 yr. We present correlations for all lags but used lags yielding maximum correlations and patterns similar to the expected pattern in subsequent analyses.

To define the optimal spatial scale at which charcoal accumulation reflects area burned, we correlated CHAR series with ten area-burned series representing fire occurrence within radii of 0.1 to 53 km from each sediment core. Ordinary least-squares regression was used to fit a linear model to each comparison, and we used the coefficient of determination (r^2) to evaluate the strength of the CHAR-area burned relationship. To test the null hypothesis of no relationship between CHAR and area burned, we used a Monte Carlo approach that accounts for autocorrelation in the charcoal and area-burned series, and non-linearity or outliers. The probability of obtaining an r^2 value equal to or greater than that observed, p, was calculated based on r^2 values from 5000 simulations representing the null hypothesis (Gotelli and Ellison, 2004). For each simulation, we used a block resampling method that shifted the start of the CHAR and area-burned records by a random number of years, wrapping samples from the end to the start of the record. Shifting, rather than scrambling, accounts for autocorrelation in each record by preserving sample ordering and is thus more conservative than using parametrically constrained p-values (Adams *et al*., 2003).

Composite fire history record and an area-burned model

Using peaks identified with optimal threshold values, we calculated fire-return intervals (FRIs; years between fires) for each record and pooled FRIs from all records, assuming they represent the same fire regime. A Weibull model [$y = f(x \mid b,c) = cb^{-c}x^{c-1}e^{-(\frac{x}{b})^c}$] was fit to the pooled distribution using maximum likelihood techniques (e.g. Clark, 1989; Higuera *et al*., 2009). Theoretically, this distribution represents the probability of a fire-return interval occurring within an area equal in size to the source area represented by charcoal *peaks* (defined by the data, below) over the entire sampling period. The Weibull b parameter is directly related to the mean and median fire-return interval (yr), while the c parameter indicates an increasing (c>1), constant (c=1) or decreasing (c<1) probability of fire with stand age (Agee, 1993).

We formed three composite CHAR records that we hypothesized would correlate with area burned for the entire study area, each including the total number of sites recording during a given interval, as follows: one site from AD 1240–1300, two from 1300–1500, and four from 1500–1975. Individual records were rescaled to range between 0 and 1 (Power *et al*., 2008) and averaged to create the composite record. We created a univariate regression model predicting area burned as a function of CHAR in the composite record for each of the 19 samples in the calibration period (AD 1675–1960). Models based on a power relationship (y=ax^b) fit with robustness criteria (Neter *et al*., 1996) explained the most variation in area burned. Models created after transforming both the charcoal and area-burned data sets were less powerful and less robust (data not shown).

To measure the skill of the regression model, we used the adjusted r^2 and reduction-of-error (RE) statistics (Fritts, 1976). The RE statistic indicates the accuracy of a model relative to the null model (i.e. the calibration period mean) and can range from $-\infty$ to 1. RE >0 indicates skill, that the regression model is a better predictor of area burned than is the null model. We calculated the RE statistic for each model and for each of 5000 cross-validations. For each cross-validation, a regression submodel was created as described above but using a subsample of ten CHAR-area burned pairs starting in randomly selected years (utilizing 53% of the complete calibration data set). As with the site-specific simulations, samples were wrapped and temporal ordering was maintained to account for autocorrelation in each record. Area burned of the remaining nine samples was predicted based on this submodel and the remaining CHAR values. As an index of robustness to new predictions, we report the median RE, RE_{median}, from these 5000 cross-validations.

Testing for climate–fire linkages

We compared reconstructed area burned with three aspects of a tree-ring-based reconstruction of annual precipitation for the Yellowstone region spanning AD 1256–1998 (Gray *et al*., 2007). First, to evaluate systematic relationships between area burned and precipitation, we calculated the correlation coefficient (Pearson and Spearman) between area burned and annual precipitation averaged over the same 15 yr intervals. Second, we compared median area burned in the intervals containing the ten driest and ten wettest years to test the null hypothesis that area burned in periods with extreme dry or wet years did not differ from the median area burned over the AD 1256–1975 period of overlap. Confidence intervals were calculated from 10 000 simulations where the relative location of the area burned, dry-year, and wet-year time series were randomly shifted (and wrapped, as in other simulations). For each simulation, the median area burned in the randomly shifted dry and wet years was calculated and recorded, and the 5th, 10th, 90th and 95th percentiles from these simulations serve as one-way 90% and 95% confidence intervals. Third, we tested the hypothesis that the area-burned time series varied significantly over c. 56–64 yr periods, the bandwidth over which the Gray *et al*. (2007) precipitation reconstruction contained significant spectral power. We estimated the power spectrum of the area-burned time series using Welch's method with a Hamming window (with a width of ten samples and 50% overlap; Welch, 1967; analysis done using Matlab software, Mathworks Inc.) and hypothesized precipitation variations near 56–64 yr p could drive area-burned patterns. We used the F statistic (with $dof_{numerator}$ = (50 samples/50 spectral estimates) * 1.2 ≈ 1, and $dof_{denominator}$ =1000) to determine the probability that variance in the area-burned power spectrum differed from that of red noise (with similar first-order autocorrelation). By increasing the number of spectral estimates to 50, we substantially reduced our statistical power, but in trade-off we gained precision in each spectral band. Interpretations of the area burned power spectrum were thus done fully within the context of our hypothesis.

Results

Calibrating charcoal records to detect fire occurrence and defining 'local' spatial scales

Accuracy was maximized when comparing tree-ring-inferred fires to charcoal peaks identified with the 95th (Dryad, Mallard, West Thumb) or 99.9th percentile threshold criterion (Duck; Table 1; Figure 2). Based on these charcoal thresholds, the signal-to-noise index (SNI) was high for Dryad, Duck, and Mallard lakes (0.90, 0.94, 0.96) and relatively low for West Thumb (0.44). The SNI quantifies the variability of charcoal peak values relative to non-peak values, and it can vary between 0 and 1, with 1 representing maximum signal and <0.5 suggesting poor separation between peak and non-peak values (Higuera *et al*., 2009).

Table 1. Calibration results for identifying fire events with charcoal peaks based on each area-burned criterion (column 1) and threshold criterion (column 2; see methods). The highest true-positive rate (Optimal TP_{rate}) and lowest false-positive rate (Optimal TP_{rate}) correspond to maximum accuracy. The distance from sediment core at which maximum accuracy is achieved identifies the optimal spatial scale for interpretations

Area-burned criterion	Threshold criterion	Site	Optimal TP_{rate}	Optimal FP_{rate}	Maximum accuracy	Distance of max. acc. (km)
4 ha (min. size resolved)	95th percentile	**DR**	**1.00**	**0.00**	**1.00**	**1.2**
		DU	1.00	0.50	0.50	1.3
		MA	0.50	0.00	0.50	0.7
		WT	**0.80**	**0.00**	**0.80**	**3.0**
	99th percentile	**DR**	**1.00**	**0.00**	**1.00**	**1.2**
		DU	1.00	0.50	0.50	1.3
		MA	0.50	0.00	0.50	0.7
		WT	0.60	0.00	0.60	3.0
	99.9th percentile	DR	1.00	0.00	1.00	3.5
		DU	**1.00**	**0.00**	**1.00**	**1.3**
		MA	0.50	0.00	0.50	0.7
		WT	0.20	0.00	0.20	3.0
10 ha	95th percentile	**DR**	**1.00**	**0.00**	**1.00**	**2.0**
		DU	0.75	0.25	0.50	2.0
		MA	0.50	0.00	0.50	0.9
		WT	**0.80**	**0.00**	**0.80**	**3.5**
	99th percentile	**DR**	**1.00**	**0.00**	**1.00**	**2.0**
		DU	0.75	0.25	0.50	2.0
		MA	0.50	0.00	0.50	0.9
		WT	0.60	0.00	0.60	3.5
	99.9th percentile	DR	1.00	0.00	1.00	4.0
		DU	1.00	0.50	0.50	0.3
		MA	0.50	0.00	0.50	0.9
		WT	0.25	0.00	0.25	3.0
100 ha	95th percentile	**DR**	**1.00**	**0.00**	**1.00**	**2.5**
		DU	0.75	0.25	0.50	2.5
		MA	**1.00**	**0.00**	**1.00**	**1.4**
		WT	0.80	0.00	0.80	4.0
	99th percentile	**DR**	**1.00**	**0.00**	**1.00**	**2.5**
		DU	0.75	0.25	0.50	2.5
		MA	**1.00**	**0.00**	**1.00**	**1.4**
		WT	1.00	0.33	0.67	3.5
	99.9th percentile	**DR**	**1.00**	**0.00**	**1.00**	**4.5**
		DU	1.00	0.50	0.50	0.7
		MA	**1.00**	**0.00**	**1.00**	**1.4**
		WT	0.50	0.00	0.50	3.5

Bold values indicate scenarios with the maximum accuracy for that site (which can occur under more than one scenario). Site codes: Dryad Lake (DR), Duck Lake (DU), Mallard Lake (MA), West Thumb of Yellowstone Lake (WT).

Maximum accuracy was affected by the area-burned criterion only in the case of Mallard Lake, where maximum accuracy increased from 0.50 to 1.00 when true fires were defined as periods with >100 ha burned. For other sites, maximum accuracy (0.80–1.00) was obtained when true fires were defined by the minimum amount of area burned (Table 1). Maximum accuracy was also more robust to alternative threshold criteria when comparing peaks with true fires defined as periods with >100 ha burned (Table 1).

Using these optimal peak thresholds, the optimal spatial scale for detecting true fires was defined by radii between 1.2 (Dryad) and 3.0 km (West Thumb) of each core (Table 1; Figure 3a). Excluding the West Thumb core, which was taken approximately 2.5 km from land (Figure 1), the optimal spatial scale was defined by radii <1.3 km (Table 1). When considering fires within shorter distances, accuracy decreased as a result of low true-positive and high false-positive rates, whereas at greater distances accuracy decreased primarily because of low true-positive rates (Figure 3a).

Correlating charcoal accumulation and area burned and defining 'extra local' spatial scales

Charcoal accumulation rates (CHAR) were significantly correlated with area burned within 1.6 to 51 km (i.e. the entire study area) of each core (Figure 1). The optimal spatial scale for area burned varied between 6.0 km (West Thumb) and 51 km (Duck Lake) with a median of 13 km (Table 2). Maximum correlations occurred when the CHAR series lagged area-burned series by 15 (Duck Lake, Mallard Lake, West Thumb) or 30 (Dryad Lake) years. Under these circumstances, CHAR explained 22–62% of the total variation in area burned at the optimal spatial scale (Table 2). At Dryad and Mallard lakes, r^2 values increased to their maxima at 13 km (0.358 and 0.616; Table 2) and decreased at greater distances, whereas this hypothesized pattern was more ambiguous at Duck Lake and West Thumb (Figure 3b). The optimal spatial scale at Duck Lake is particularly ambiguous, given it had the lowest r^2 values of all sites (0.216; Table 2) and little variation between radii of 3.2 and 51 km (Figure 3b).

Composite fire-history records and area-burned model

Using the optimal peak thresholds, 25 fire-return intervals (FRI) from the pooled data set varied between 30 and 270 yr, with a mean and median (95% CI) of 78 (59–102) and 60 (53–75) yr. The distribution of FRIs was fit by a Weibull model with b (yr) and c (unitless) parameters of 89 (67–114) and 1.61 (1.36–2.54) (Kolmogorov-Smirnov goodness-of-fit test: $k = 0.24$, $p = 0.08$).

Composite CHAR records were significantly correlated with area burned over the calibration period (AD 1675–1960), with

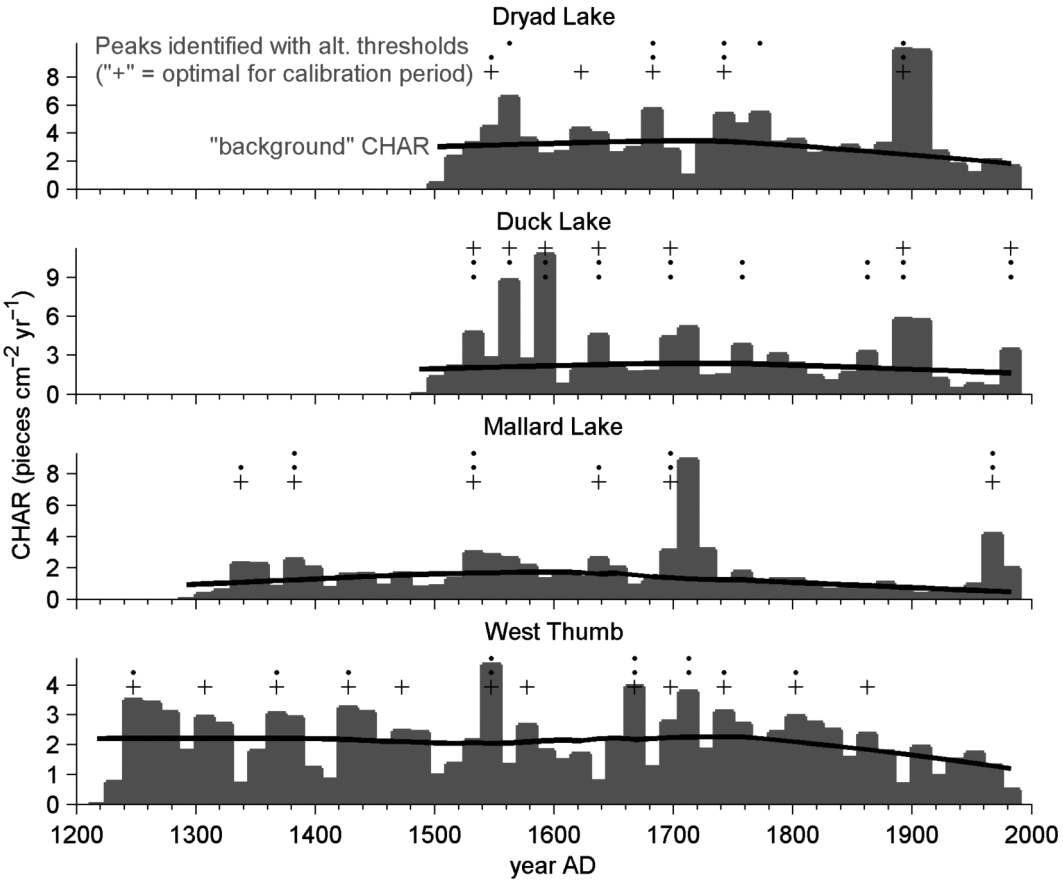

Figure 2. Interpolated records of charcoal accumulation rates (CHAR) from Dryad Lake, Duck Lake, Mallard Lake, and West Thumb. Threshold values identify peaks exceeding 'background' CHAR (black line) by a given value. Peaks identified based on the three different threshold criteria are identified by '·' or '+', with the latter indicating the maximizing accuracy for the calibration period (i.e. the 'optimal threshold value')

variations in CHAR explaining 59–79% of the variation in area burned (Table 3, Figure 4). Each model had a positive RE statistic (0.46–0.78) that was robust to cross-validation procedures (RE_{median} = 0.52–0.67; Table 3, Figure 5c). The composite record based on four sites explained the most variation in area burned (79%) and was the most robust (RE_{median} = 0.67). Models based on two and one site(s) explained less variation (59 and 64%) and were less robust (RE_{median} = 0.52 and 0.65; Table 3; Figure 5b,c). For each model, variability in CHAR during the calibration period spanned the full range of variability for the entire reconstruction, eliminating the need for extrapolation beyond the calibration period (e.g. Figure 5e). The final area-burned reconstruction utilized the three different regression models, spanned AD 1225–1975, and varied between 220 and 21 190 ha burned in any 15 yr interval (Figure 5). Large areas burned (>10 000 ha) in the mid-thirteenth century, *c*. AD 1530, and *c*. AD 1700, and smaller areas burned (*c*. 5000 ha) around AD 1300, 1375, 1420, 1580, 1660, 1750, and 1875 (Figure 5e).

Testing for climate–fire linkages

Reconstructed area burned was uncorrelated with reconstructed precipitation (Gray *et al*., 2007) for the period of overlap (Spearman r^2 = 0.05, p = 0.13; Pearson r^2 = 0.04, p = 0.14; Figure 5d,e). However, median area burned during periods including the ten driest years in the Gray *et al*. (2007) data set (5176 ha) was significantly higher than median area burned over the entire AD 1258–1975 period of overlap (p=0.05; 2908 ha; Figure 5d,e, Figure 6a). During periods including the ten wettest years, median area burned (2792 ha) did not differ from that for the period of overlap (Figure 6a). Finally, the power spectrum of the entire area-burned reconstruction exceeded the 95% confidence interval from a period of 56–58 yr (Figure 6b). Although not hypothesized *a priori*, the area-burned power spectrum also exceeded the 90% confidence interval at a period of 150 yr.

Discussion

Reconstructing fire regimes with sediment-charcoal records

Identified charcoal peaks most accurately reflected large, high-severity fires relatively close (1–3 km radii) to coring locations. This optimal spatial scale is slightly larger than the 0.5–1.0 km inferred from previous empirical and theoretical work (e.g. Gavin *et al*., 2003; Higuera *et al*., 2007), but the result is influenced somewhat by the limitations of the tree-ring record. Even within the optimal spatial scale, some fires failed to leave detectable peaks in the sediment record, as indicated by the low true-positive rates and less-than-perfect accuracy (Figure 3). Fire signatures were undoubtedly influenced by aspects other than distance-from-lake, including fire size, fire intensity, fire severity, and

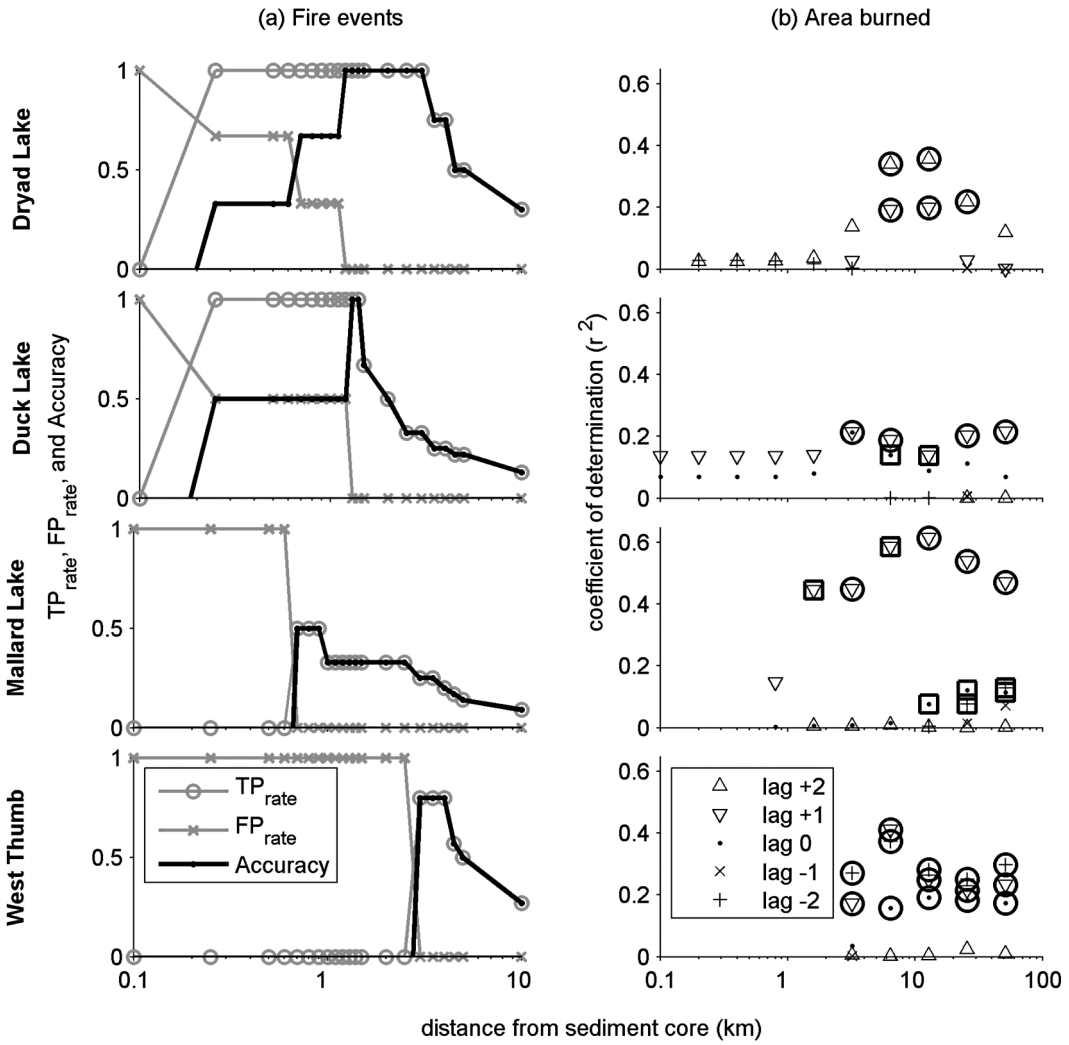

Figure 3. Spatial scale of charcoal records for reconstructing individual fire events and area burned. (a) Trade-offs between the true-positive rate (TP_{rate}) and false-positive rate (FP_{rate}) when comparing charcoal peaks to all tree-ring-inferred fires within different distances of each sediment core. Analysis is based on the all fires > 4 ha (the minimum size resolved) and the 95th- (Dryad, Duck, Mallard lakes) or 99.9th- (West Thumb) percentile threshold criterion for identifying charcoal peaks. Accuracy is the difference between the TP_{rate} (proportion of peaks correctly identifying fires) and FP_{rate} (proportion of peaks incorrectly identifying fires) and is maximized at distances between 0.7 (Mallard Lake) and 4.0 (West Thumb) km from a sediment core. (b) Coefficient of determination (r^2) for comparisons between CHAR and area-burned time series including fires at different distances from each sediment core. Symbols identify different lag values, in 15 yr time steps, of CHAR relative to area-burned series. For example, 'lag +1' indicates comparisons between area burned in the bin centered on year *t* to CHAR in the bin centered on year *t*+15. Circles (squares) surround r^2 values statistically significant at the alpha = 0.05 (0.10) level. For each lake, symbols are shown only for positive correlations (there were no significant negative correlations). Note: For both (a) and (b), the West Thumb core is approximately 2.5 km from land and thus cannot detect area burned at closer distances (Figure 1)

wind direction (Duffin *et al*., 2008; Gardner and Whitlock, 2001; Higuera *et al*., 2005). We did not quantify fire severity and wind direction, but accuracy was more robust to different peak thresholds and higher, in some cases, when fire occurrence was defined as fires >100 ha (Table 1). This finding supports the assumption that larger fires introduce more charcoal to a lake than small fires and create large charcoal peaks suitable for decomposition methods (Higuera *et al*., 2007; Whitlock *et al*., 2006). The fact that the sediment core from West Thumb, a basin orders of magnitude larger than the other sites, detected fires with reasonable accuracy (0.8; Figure 3a) suggests that basin size in itself does not preclude detecting fires close to the lake shore (Carcaillet *et al*., 2007). The low signal-to-noise index (SNI) for West Thumb, however, indicates that identifying individual peaks in this record is questionable, because there is little variation between peaks and non-peak values. This feature of the record likely reflects the basin's large size, which limits the minimum distance-to-fire for a coring location and thus reduces the magnitude of the charcoal peaks associated with local fires. Because the sediments of the West Thumb core are laminated, the low SNI in this record cannot be accounted for by sediment mixing. A full evaluation of the relationship between basin size and charcoal peak variation or the charcoal source area is beyond the scope of this study.

Although charcoal peaks reflect fire occurrence within a 1–3 km radius, total charcoal accumulation reflected area burned at larger spatial scales. At all sites, the charcoal accumulation rate (CHAR) was significantly correlated with area burned at distances from 10^0–10^1 km, up to an order of magnitude greater than distances defining the optimal spatial scale for peak-inferred fires. In most cases, and particularly at Dryad and

Table 2. Calibration results for reconstructing area burned with total charcoal accumulation. Maximum correlation (r_{max}) between charcoal accumulation and area burned is stratified by lead-lag value and site, with corresponding distance from coring site for each correlation

Lead-lag value	Site	r_{max}	r^2_{max}	p (r^2_{max})	Distance of r^2_{max} (km)
2	**DR**	**0.598**	**0.358**	***0.005***	**13**
	DU	0.036	0.001	0.283	51
	MA	0.099	0.010	0.173	6
	WT	0.157	0.025	0.299	26
1	DR	0.446	0.199	0.197	13
	DU	**0.465**	**0.216**	***0.006***	**51**[a]
	MA	**0.785**	**0.616**	***0.012***	**13**
	WT	**0.641**	**0.411**	***0.043***	**6**
0	DR	−0.027	0.001	0.436	26
	DU	0.462	0.213	***0.040***	**3**
	MA	0.349	0.122	0.103	26
	WT	0.437	0.191	0.101	13
−1	DR	0.053	0.003	0.471	26
	DU	0.078	0.006	0.308	26
	MA	0.267	0.071	0.202	51
	WT	0.040	0.002	0.379	3
−2	DR	0.168	0.028	0.863	0.4
	DU	0.026	0.001	0.389	6
	MA	0.358	0.128	**0.098**	51
	WT	0.612	0.374	***0.017***	6

[a]For the lag +1 scenario at Duck Lake, $r^2 = 0.2139$ ($p < 0.10$) for comparisons within 3.2 km of the core.
p-values < 0.10 are bold, < 0.05 are bold italic, and < 0.01 are underlined bold italic. The lead-lag value with the maximum correlation for each site is bold across all columns. Site codes are listed in Table 1.

Table 3. Alternative regression models relating charcoal accumulation in a composite record to area burned from AD 1675 to 1960 (n = 19). Positive reduction of error (RE) values indicate that the model is a better predictor of area burned than the mean of the series alone (i.e. the model has skill). Cross-validation involved constructing 5000 models based on a random subset of data points (53%) and then calculating the RE statistic for predictions using data excluded from the model (see methods)

Sites contributing	Model: $y = ax^b$	F-stat	p	r^2	r^2_{adj}	RE	Cross-validation RE_{median}
DU, DR, MA, WT	a = 60202; b = 2.250	93.31	0.0000	0.80	0.79	0.78	0.67
MA, WT	a = 25950; b = 1.711	40.55	0.0000	0.61	0.59	0.46	0.52
WT	a = 70780; b = 4.936	36.50	0.0000	0.66	0.64	0.53	0.65

Site codes are listed in Table 1.

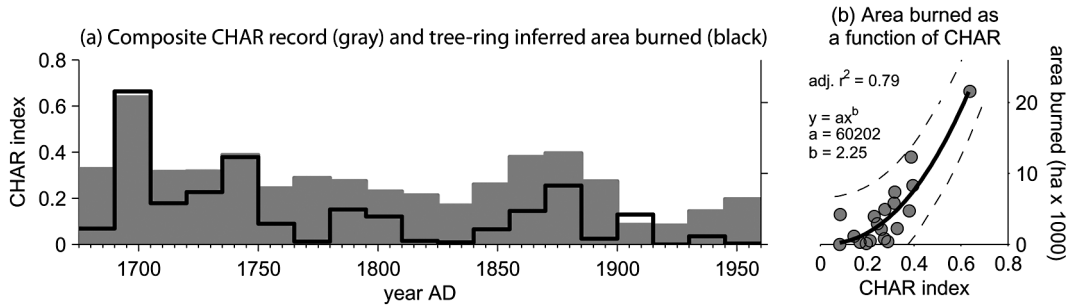

Figure 4. Comparison between the four-site composite charcoal record and area burned within the entire study. (a) Composite charcoal record, expressed as a charcoal accumulation rate (CHAR) index (gray bars, left y-axis), and area burned (thick line, far right y-axis) for the AD 1675–1960 calibration period. (b) Scatter plot of area burned as a function of CHAR from the two series in (a) with the best-fit power model and adjusted r^2 statistic. Dashed lines represent 90% confidence intervals for new predictions

Mallard lakes, correlations increased to a distinct maximum (between 6 and 51 km) and then decreased as the CHAR no longer explained the addition of area burned from greater distances (Figure 3b). These patterns are strikingly similar to results from the CharSim using large charcoal dispersal distances (10^0–10^1 km; figure 7 in Higuera *et al*., 2007). In simulations, the distance of maximum correlation was defined by the size of the potential charcoal source area (PCSA, the area from which all airborne charcoal reaching a lake originates). Our results thus imply that the PCSA for macroscopic charcoal in our study area is on the order of 10^0–10^1 km from a lake, although more precise estimates require a larger tree-ring fire-history data set (discussed below). Source areas defined by radii in the 10^1 km range may be independent of (or robust to) fuel types. For example, significant correlations between macroscopic charcoal (>150 μm) and area burned were noted at distances up to 20 km in a study from African savanna (Duffin, 2008), implying similar charcoal transport distances in grassland

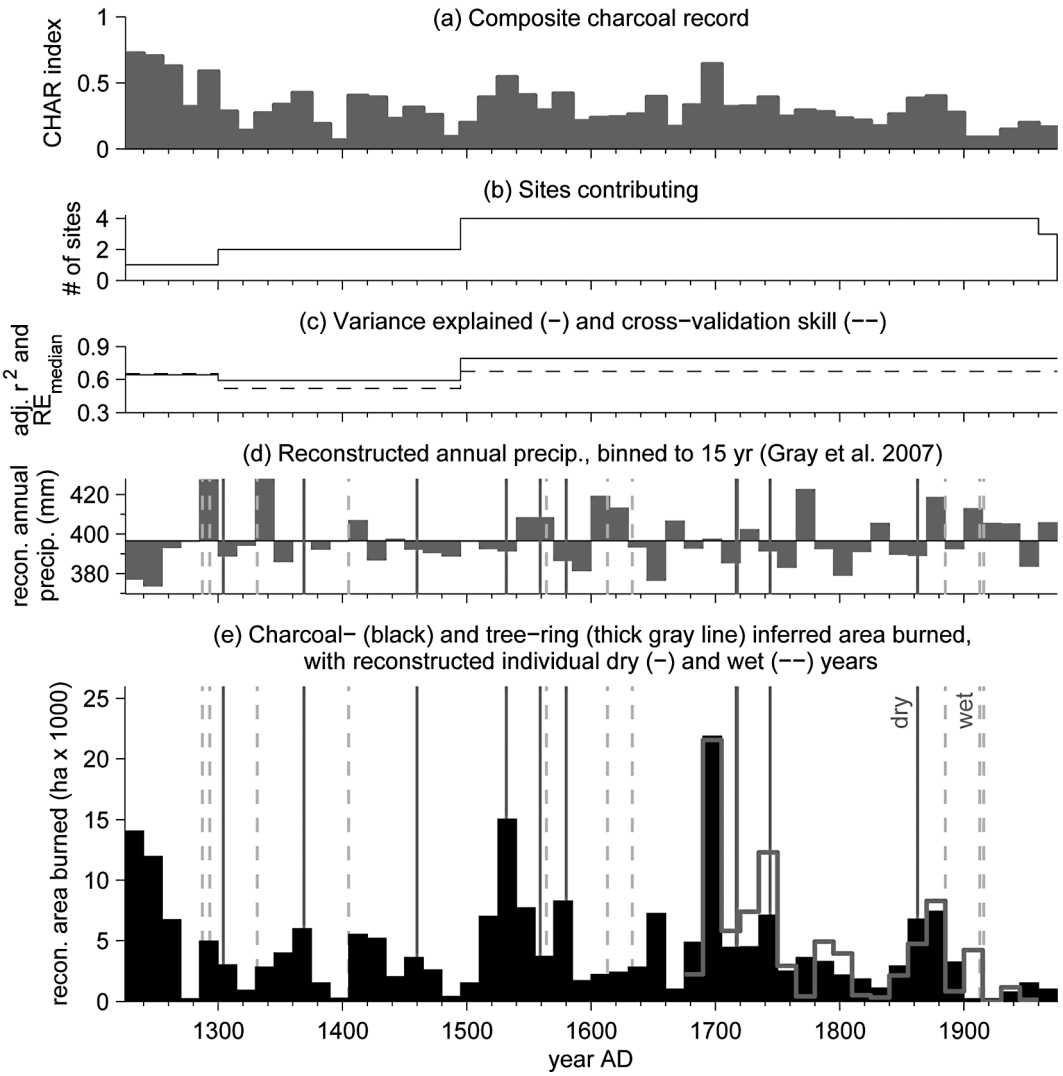

Figure 5. Summary charcoal-based fire history for the study area compared with dry and wet years from the Gray *et al.* (2007) precipitation reconstruction. (a) Composite charcoal record expressed as a charcoal accumulation rate (CHAR) index from AD 1225–1975; (b) the number of sites contributing to the composite record; (c) variation in area burned during the calibration period explained by the composite record used in each model (r^2) and the median RE value from cross-validations (RE_{median}); (d) reconstructed annual precipitation for the Yellowstone National Park (YNP) region, binned into 15 yr intervals corresponding to the CHAR record (Gray *et al.*, 2007); and (e) reconstructed area burned (dark bars), tree-ring-inferred area burned (thick gray line) during the AD 1675–1960 calibration period, and the ten driest (vertical solid line) and ten wettest (vertical dashed line) years from AD 1258 to 1998 from the Gray *et al.* (2007) precipitation reconstruction. Note: Gray *et al.* identify AD 1258 as the start of 'the best replicated portion' of their reconstruction and do not include earlier years in the list of driest and wettest years

systems as in our pine-dominated study area. Both examples add support to theoretical (Higuera *et al.*, 2007; Peters and Higuera, 2007) and empirical (Gardner and Whitlock, 2001; Hallett *et al.*, 2003; Pisaric, 2002; Tinner *et al.*, 2006) studies suggesting that even macroscopic charcoal (>150 μm diameter) in lake sediments comes from within tens of kilometers. Dispersal distances at this scale are similar to pollen dispersal distances for many coniferous taxa (Jackson and Lyford, 1999), and the similarity may explain why pollen and macroscopic charcoal data often show similar variations through time (Larsen and MacDonald, 1998; Marlon *et al.*, 2006). In contrast, variations in fire frequency, based on time series of charcoal peaks, generally bear little correspondence to changes in pollen data (Tinner *et al.*, 2008; Whitlock *et al.*, 2008), probably because charcoal peaks reflect fires within one to several kilometers of the lake, whereas pollen data register vegetation at larger spatial scales (Jackson and Lyford, 1999; Sugita, 1993, 2007).

A key implication of our CHAR-area burned correlations is that variations in CHAR offer a large-scale, moderately precise metric of fire history. This correlation is an implicit assumption at the foundation of recent studies synthesizing networks of charcoal records to infer large-scale patterns in biomass burning (Marlon *et al.*, 2006, 2008, 2009; Power *et al.*, 2008), but to date it has little empirical support (Duffin *et al.*, 2008; Enache and Cumming, 2006; Tinner *et al.*, 1998) and to our knowledge has not been demonstrated in composite records. Our regression model illustrates that area burned can be quantified based on charcoal accumulation, and in this study our composite record explained 79% of the variability in area burned in the study area (Table 1; Figures 3b, 4). Even the model based on one lake provided reasonable results, although explanatory power and skill increased as more sites were included (Table 3). The improvement likely reflects the diminishing influence of site-specific variables unrelated to fire occurrence (e.g. basin characteristics,

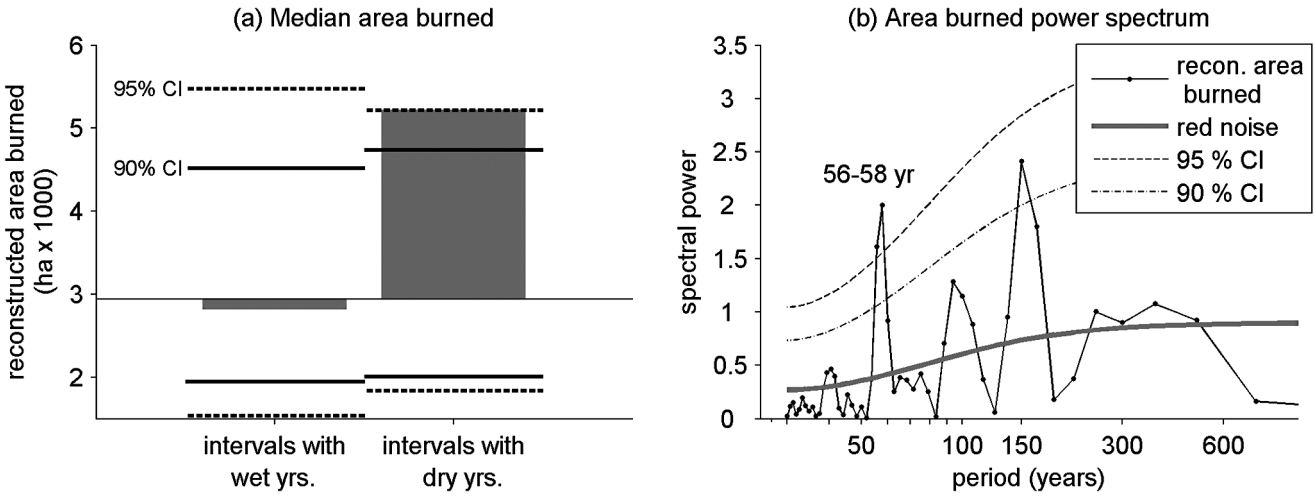

Figure 6. Evidence of climate-fire linkages in the area burned reconstruction. (a) Median area burned for periods with wet and dry year(s) in the Gray *et al.* (2007) precipitation data set. Median area burned in periods including extreme wet years (2792 ha) did not differ significantly from the series-wide median; median area burned in periods including extreme dry years (5176 ha) was significantly higher than the series-wide median (2908 ha), defined by the period of overlap with the precipitation data (AD 1258–1975). Confidence intervals were based on 10 000 simulations where the area burned and dry- and wet-year time series were randomly shifted to test the null hypothesis of no difference in median area burned among dry, wet, and random years (see Methods). (b) Power spectrum of the area burned reconstruction for the entire AD 1225–1975 period. Confidence intervals (CI) indicate the expected variance in spectral power around the null model of red noise (thick gray line). The area-burned reconstruction contains significant variability at 56–58 yr periods, similar to periods of significant variability in the precipitation reconstruction for YNP region spanning AD 1258–1998 (56–64 yr; Gray *et al.*, 2007)

local vegetation, and charcoal taphonomy), and it points to the value of including multiple records in area-burned reconstructions. Ideally, a reconstruction would be based on similar sites equally spaced throughout the calibration study area, so that the entire area could be sampled based on estimates of the optimal spatial domain from charcoal-area burned correlations. As with most methods based on lake-sediment charcoal, this approach assumes that a charcoal record is dominated by airborne deposition, or that the temporal scale of redeposition is accounted for by the sampling resolution.

Although we found strong correspondence between charcoal and tree-ring inferred fire occurrence and area burned, several limitations of the charcoal and tree-ring records constrain our interpretations. First, the tree-ring reconstruction represents only one realization of fire history in space and time, which limited estimates of optimal spatial scales from comparisons of charcoal peaks and known fires. For example, maximum accuracy could occur at shorter distances (Table 1), but detection would require historical fires in closer proximity to each lake than actually occurred. Extensive areas of water around some coring sites (e.g. Dryad Lake and West Thumb, Figure 1) also precluded local fires. The optimal spatial scales for fires detected with charcoal peaks, therefore, should be taken as maximum estimates. Second, the spatial extent and accuracy of the tree-ring record affected estimates of the optimal spatial scales for fire detection and area burned. Fires beyond the study area undoubtedly deposited charcoal in each lake, but these events could not be included in our analyses because of the spatial extent of the tree-ring record. That we still achieved reasonable accuracy and correlations may reflect spatial autocorrelation between the fire history inside and directly outside the study area. However, missing and/or imprecise fire-history information likely accounted for at least part of the unexplained variance in both the site-specific and composite models relating charcoal accumulation and area burned. An independent area-burned record extending to *c.* 50 km of each lake would be required to more accurately estimate the optimal spatial scale of area-burned correlations and potential charcoal source areas (PCSA; Higuera *et al.*, 2007). For West Thumb in particular, the optimal spatial scale for recording area burned (6 km) was likely artificially low. Given the basin size of West Thumb and its location at the edge of the study area, charcoal accumulation at this site probably reflects area burned outside the study area. Finally, the tree-ring and CHAR data likely contain temporal errors that confound charcoal–fire comparisons. For example, the stand-age data reflect a short but varying time between fires dates and tree regeneration, although binning stand ages in 15 yr intervals reduced this potential error. Charcoal accumulation may also lag a fire event by several years (Duffin *et al.*, 2008; Whitlock and Millspaugh, 1996). Unknown errors in the ^{210}Pb chronologies and extrapolated dates are also an important source of uncertainty potentially leading to inaccurate sedimentation rates and chronologies. We found the best correlations between CHAR and area burned when charcoal records lagged area-burned records by 15–30 yr (Figure 3b). These optimal lags are consistent with mechanisms of charcoal taphonomy leading to delayed deposition at a coring location (Duffin *et al.*, 2008; Whitlock and Millspaugh 1996), but they may also reflect chronological errors that vary within and between records. Such chronological errors likely account for some portion of the unexplained variance in the area-burned regression models, even after optimal lags were used.

Fire history in central Yellowstone National Park

Climatic and vegetational controls have interacted to determine local-scale and large-scale fire history in central Yellowstone National Park (YNP) over the past seven centuries. In this remote part of YNP, prehistoric and recent human activities are thought to have been of little consequence (Knight 1991; Romme and Despain, 1989).

Our results suggest that climate variability was an overriding factor determining large-fire occurrence, regardless of ignition patterns. Climate controls are highlighted by two aspects of our reconstruction. First, increased area burned coincident with the ten most extreme drought years since AD 1250 (Figure 6a) suggests that summer drought promoted above-average burning. Presumably, this was through drying the abundant, typically moist fuels that characterize subalpine forests (Renkin and Despain, 1992; Schoennagel *et al*., 2004), creating flammable conditions and increasing the probability of fire ignition and spread. Large fires in subalpine forests across the Rocky Mountains (Schoennagel *et al*., 2005; Sibold and Veblen, 2006), within YNP (Balling *et al*., 1992), and within the Central Plateau study area (Schoennagel *et al*., 2005) have been linked to annual-scale drought over the past several decades to centuries. Our area-burned reconstruction provides direct evidence that these mechanisms have been in place for the last 750 yr. Importantly, reconstructed area burned was not correlated with 15 yr average annual precipitation. Although this may reflect imprecision in either reconstruction, it is consistent with the overriding importance of annual climate conditions in determining fire occurrence as compared with 15 yr averages (Balling *et al*., 1992). Notably, our ability to detect links between above-average area burned and annual drought was wholly dependent on having an annual-scale precipitation reconstruction, even though area burned was reconstructed at 15 yr intervals.

A second aspect of the central YNP fire history suggests that climate influences fire occurrence in subalpine forests over longer, multidecadal timescales. Significant variation in area burned at *c*. 60 yr periods (Figure 6b) and a study-area-wide median fire-return interval (FRI) of 60 yr (95% CI: 53–75) overlap with the scale of significant variability in reconstructed precipitation from AD 1250 to 1975 (56–64 yr; Gray *et al*., 2007). Variation in climate and fire at similar timescales suggests that annual-scale linkages, while not conserved at 15 yr periods, are either conserved or reappear at multidecadal timescales. Long-term moisture deficits could favor fire occurrence by increasing tree mortality and thus surface fuels (Bigler *et al*., 2005; Tinner *et al*., 2008), and/or by increasing the frequency of extreme dry, fire-conducive conditions at annual and subannual timescales (Gray *et al*., 2007). This hypothesis is supported by two key multidecadal precipitation anomalies in the YNP precipitation record. A multidecadal drought in the mid-thirteenth century, also reflected in regional drought reconstructions (Cook *et al*., 2004), corresponds to a 30 yr period with >25 000 ha burned. Gray *et al*. (2007) hypothesized that this period likely favored widespread disturbance in YNP, including forest fires, and ecological reorganization. Additionally, a multidecadal wet period in the early twentieth century, again reflected in the regional reconstructions (Gray *et al*., 2004; Woodhouse *et al*., 2006), coincides with 45 yr with < 2000 ha burned (Figure 5e).

Although climate has clearly determined central YNP fire regimes at multiple time scales (Millspaugh *et al*., 2000; Schoennagel *et al*., 2005; this study), our reconstruction points to the importance of non-climatic factors as well. Composite fire-return intervals suggest an increasing probability of fire with stand age (Weibull *c* parameter estimate > 1, 95% CI: 1.36–2.52), implying that post-fire fuel accumulation mediates direct links between climate and local-scale fire occurrence over decadal timescales. Although charcoal records have a minimum detectable fire-return interval (FRI; 30 yr in this study, $n = 4$ of 26), the fact that the modal FRI in this study was 60 yr ($n = 9$ of 26) suggests increased probability of burning with stand age was not an artifact of the charcoal data. Stand age significantly affected area burned in YNP in recent decades, with the greatest proportion of crown fires in lodgepole pine stands in mid- to late-successional stages (150–300+ yr; Renkin and Despain, 1992). When the landscape is dominated by mid- to late-successional stands, fuel structure and continuity serve to promote fire spread across broad areas, as in AD 1988 (Turner *et al*., 1994) when high-severity forest fires burned 25 000 ha in the study area (National Park Service, unpublished data, available online: http://science.nature.nps.gov/nrdata/; see also Turner *et al*., 1994). Although the 1988 fires are unprecedented in light of our reconstruction, a similar combination of stand development and favorable fire weather and climate was likely responsible for widespread burning (>10 000 ha) in *c*. AD 1240, 1540, and 1700 (Romme and Despain, 1989; this study, Figure 5e). Our reconstruction and the AD 1988 fires indicate that the large fire events have occurred at 150–300 yr intervals over the past 750 yr. This 150 yr period is also a period of moderately significant ($p<0.10$) variability in the area-burned power spectrum, although this was not hypothesized *a priori* (Figure 6b). Variability at these timescales is consistent with the timing of post-fire stand development leading to an increased probability of crown fires (Renkin and Despain, 1992). Thus, modern fire observations and fire-history records from both tree-ring (Romme, 1982) and sediment-charcoal (this study) data suggest that the most extensive fires in the lodgepole pine forests of YNP arise from interactions between climate on multiple timescales, and fuel conditions, varying on decadal to centennial timescales. The interactive effects of climate and post-fire fuel accumulation on fire occurrence are not unique to subalpine forests. Similar mechanisms have been inferred in low-severity fire regimes in red pine stands of northwestern Minnesota (Clark, 1988a). In both Minnesota and central YNP, neither climate nor post-fire fuel accumulation alone fully explains local or extra-local fire activity on decadal to centennial timescales.

Conclusions

Charcoal records fill an important gap in our understanding of fire ecology and the controls of fire regimes, particularly where infrequent, stand-replacing fires limit the length of tree-ring reconstructions. In these ecosystems, charcoal records have the unique ability to reveal the role of both climatic and non-climatic factors in controlling fire activity over a range of scales. Over centennial-to-millennial timescales, individual charcoal peaks register fire occurrence within hundreds of meters to a few kilometers of a site, providing 'local' records valuable for studying site-specific fire history. Charcoal accumulation in lake sediments registers fires from larger areas and can provide quantitative reconstructions of area burned at regional spatial scales, i.e. within several to tens of kilometers of a site. Combining peak-inferred fire-return intervals (Gavin *et al*., 2006; Higuera *et al*., 2009) and total charcoal accumulation in composite records (Brubaker *et al*., 2009; Marlon *et al*., 2006, 2008, 2009; Whitlock *et al*., 2008) allows inferences at even larger spatial scales and is promising for detecting climate–fire linkages.

In the case of YNP, our area-burned reconstruction facilitated comparisons with reconstructed annual precipitation and suggest that widespread burning in the past was likely determined by annual to multidecadal variations in drought, as well as the

centennial-scale patterns of stand development and associated fuel accumulation. These factors combined to produce at least three periods of widespread burning in the study area (> 10 000 and up to 21 000 ha) within the past 750 yr. Historical evidence linking drought with large areas burned is consistent with predictions of increased area burned under future climate warming (Littell *et al*., 2009; Westerling *et al*., 2006), but as forest communities in YNP respond to climate change (Bartlein *et al*., 1997; Schrag *et al*., 2008), current links between climate, vegetation, and fire will also be altered. The degree to which future fire regimes are determined solely by climate or by a combination of climate and vegetation change will depend upon the nature, pattern, and rate of vegetation change.

Acknowledgments

We thank Sarah Millspaugh for providing charcoal data, Daniel Tinker and Bill Romme for providing the stand-age data, and Stephen Gray for providing the YNP precipitation reconstruction. Stephanie Mumma and Whitney Brawner helped with data preparation and preliminary analysis. Earlier drafts of the manuscript were improved by comments from Dan Gavin, Steven Jackson, Ryan Kelly, Bill Romme, Willie Tinner, and three anonymous reviewers.

Funding

Funding was provided by a National Park Ecological Research Fellowship (PEH), the Yellowstone Center for Resources and National Science Foundation EAR-0818467 (CW).

Appendix A. Supporting Figures

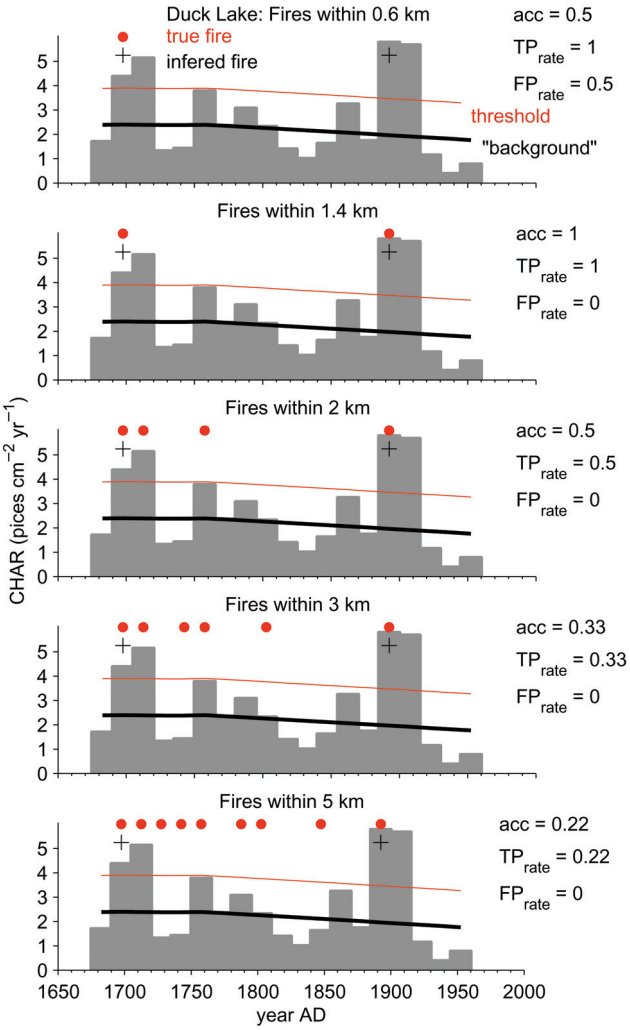

Figure A1. Example illustrating how accuracy is defined by comparing peak-inferred fires to periods when area burned within different distances from Duck Lake. The charcoal accumulation rate (CHAR; gray solid bars), background CHAR (thick line), threshold used to identify peaks (thin line), and peaks exceeding the threshold (black '+' symbols) do not vary between panels, but the number of true fires (gray circles) increases with distance from lake (from top to bottom panel). Within close distances to the lake (e.g. 0.6 km, top panel), one of two inferred fires is not matched by a true fire, resulting in a false-positive rate (FP_{rate}) of 0.50. The single true fire is matched with an inferred fire, resulting in a true-positive rate (TP_{rate}) of 1.00. As the number of true fires increases with distance-from-lake, the FP_{rate} decreases. When considering fires within 1.4 km (second panel from top), the FP_{rate} reaches zero while the TP_{rate} remains at one, representing perfect accuracy. Beyond this distance the TP_{rate} decreases as more true fires are included in the comparison. Note: for these comparisons the charcoal record is shown only for periods where it overlaps with the tree-ring record (1675–1960)

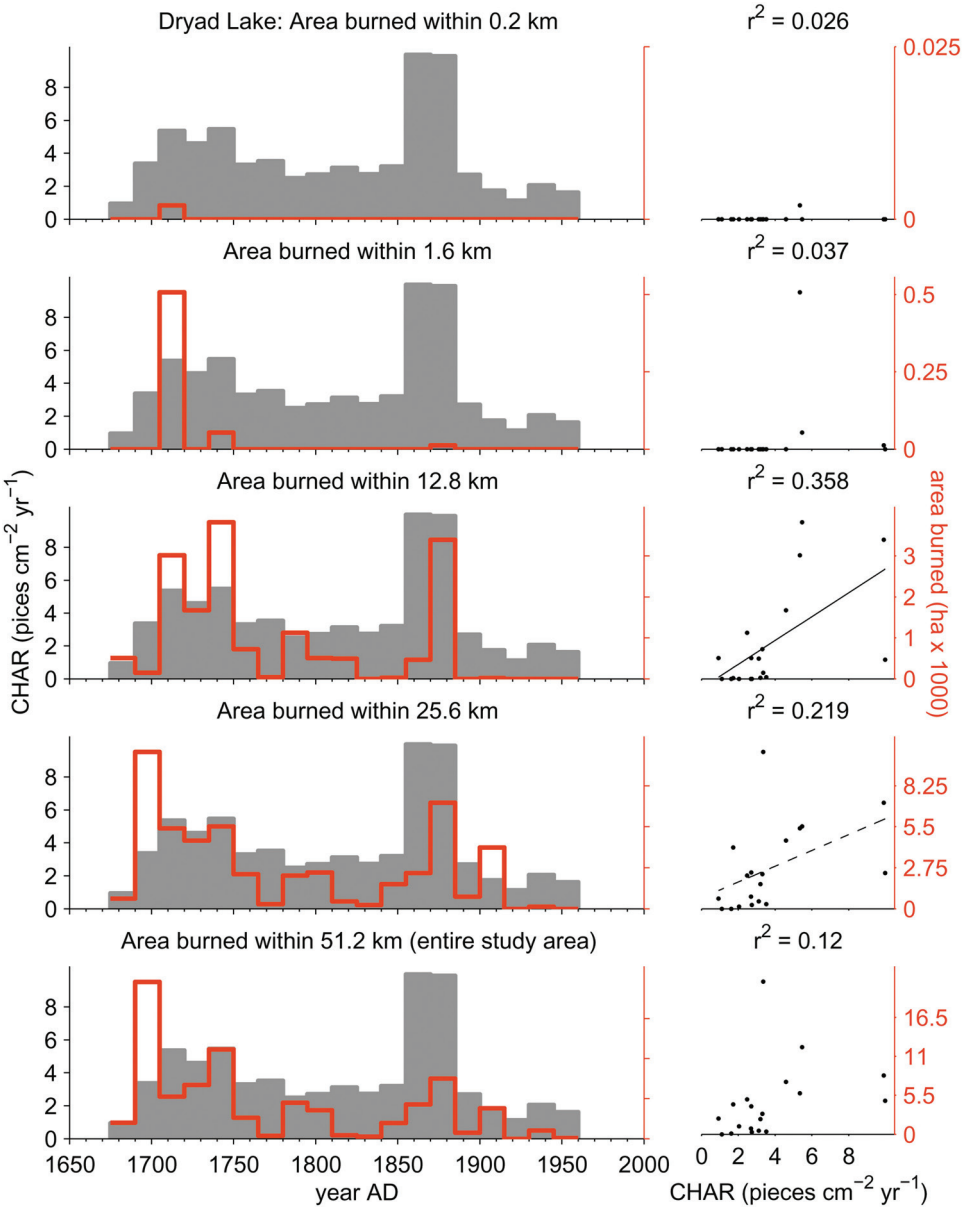

Figure A2. Example illustrating relationships between charcoal accumulation rate (CHAR) and area burned within different distances from Dryad Lake. Left column: The charcoal record (gray bars) does not vary between panels, but the record of area burned (thick dark line, far right y-axis) changes as distance-from-lake increases (from top to bottom panel). Right column: scatter plots of area burned as a function of CHAR corresponding to the two series in the same row of the left column. The coefficient of determination, r^2, is noted at the top of each panel, and a solid (dashed) line is fit to the scatter plot if the relationship is significant at alpha = 0.05 (0.10). Note: this example illustrates the best match between Dryad Lake and the area burned time series, which occurs when the charcoal record lags the area burned record by two samples (30 yr; Table 2). Thus, the charcoal series is offset from its original location in time by two time steps (i.e. compare to Fig. 2 in main text)

References

Adams JB, Mann ME and Ammann CM (2003) Proxy evidence for an El Nino-like response to volcanic forcing. *Nature* 426: 274–278.

Agee JK (1993) *Fire Ecology of Pacific Northwest Forests*. Washington DC: Island Press.

Appleby PG and Oldfield F (1978) The calculation of 210Pb dates assuming a constant rate of supply of unsupported 210Pb to the sediment. *Catena* 5: 1–8.

Balling RC, Meyer GA and Wells SG (1992) Relation of surface climate and burned area in Yellowstone National Park. *Agricultural and Forest Meteorology* 60: 285–293.

Bartlein PJ, Whitlock C and Shafer SL (1997) Future climate in the Yellowstone National Park region and its potential impact on vegetation. *Conservation Biology* 11: 782–792.

Bigler C, Kulakowski D and Veblen TT (2005) Multiple disturbance interactions and drought influence fire severity in Rocky Mountain subalpine forests. *Ecology* 86: 3018–3029.

Brubaker LB, Higuera PE, Rupp TS, Olson MA, Anderson PM and Hu FS (2009) Linking sediment-charcoal records and ecological modeling to understand causes of fire-regime change in boreal forests. *Ecology* 90: 1788–1801.

Carcaillet C, Perroux AS, Genries A and Perrette Y (2007) Sedimentary charcoal pattern in a karstic underground lake, Vercors massif, French Alps: Implications for palaeo-fire history. *The Holocene* 17: 845–850.

Clark JS (1988a) Effects of climate change on fire regimes in northwestern Minnesota. *Nature* 334: 233–235.

Clark JS (1988b) Particle motion and the theory of charcoal analysis: Source area, transport, deposition, and sampling. *Quaternary Research* 30: 67–80.

Clark JS (1989) Ecological disturbance as a renewal process: Theory and application to fire history. *Oikos* 56: 17–30.

Clark JS, Royall PD and Chumbley C (1996) The role of fire during climate change in an eastern deciduous forest at Devil's Bathtub, New York. *Ecology* 77: 2148–2166.

Conedera M, Tinner W, Neff C, Meurer M, Dickens AF and Krebs P (2009) Reconstructing past fire regimes: Methods, applications, and relevance to fire management and conservation. *Quaternary Science Reviews* 28: 555–576.

Cook ER, Woodhouse CA, Eakin CM, Meko DM and Stahle DW (2004) Long-term aridity changes in the western United States. *Science* 306: 1015–1018.

Despain DG (1990) *Yellowstone Vegetation: Consequences of Environment and History in a Natural Setting*. Boulder CO: Roberts Rinehart.

Duffin KI (2008) The representation of rainfall and fire intensity in fossil pollen and charcoal records from a South African savanna. *Review of Palaeobotany and Palynology* 151: 59–71.

Duffin KI, Gillson L and Willis KJ (2008) Testing the sensitivity of charcoal as an indicator of fire events in savanna environments: Quantitative predictions of fire proximity, area and intensity. *The Holocene* 18: 279–291.

Enache MD and Cumming BF (2006) Tracking recorded fires using charcoal morphology from the sedimentary sequence of Prosser Lake, British Columbia (Canada). *Quaternary Research* 65: 282–292.

Fritts HC (1976) *Tree Rings and Climate*. London: Academic Press.

Gardner JJ and Whitlock C (2001) Charcoal accumulation following a recent fire in the Cascade Range, northwestern USA, and its relevance for fire-history studies. *The Holocene* 11: 541–549.

Gavin DG, Brubaker LB and Lertzman KP (2003) An 1800-year record of the spatial and temporal distribution of fire from the west coast of Vancouver Island, Canada. *Canadian Journal of Forest Research* 33: 573–586.

Gavin DG, Hu FS, Lertzman K and Corbett P (2006) Weak climatic control of stand-scale fire history during the late Holocene. *Ecology* 87: 1722–1732.

Gotelli NJ and Ellison AM (2004) *A Primer of Ecological Statistics*. Sunderland MA: Sinauer Associates, Inc.

Gray ST, Fastie CL, Jackson ST and Betancourt JL (2004) Tree-ring-based reconstruction of precipitation in the Bighorn Basin, Wyoming, since 1260 AD. *Journal of Climate* 17: 3855–3865.

Gray ST, Graumlich LJ and Betancourt JL (2007) Annual precipitation in the Yellowstone National Park region since AD 1173. *Quaternary Research* 68: 18–27.

Hallett DJ, Lepofsky DS, Mathewes RW and Lertzman KP (2003) 11,000 years of fire history and climate in the mountain hemlock rain forests of southwestern British Columbia based on sedimentary charcoal. *Canadian Journal of Forest Research* 33: 292–312.

Higuera PE, Sprugel DG and Brubaker LB (2005) Reconstructing fire regimes with charcoal from small-hollow sediments: A calibration with tree-ring records of fire. *The Holocene* 15: 238–251.

Higuera PE, Peters ME, Brubaker LB and Gavin DG (2007) Understanding the origin and analysis of sediment-charcoal records with a simulation model. *Quaternary Science Reviews* 26: 1790–1809.

Higuera PE, Brubaker LB, Anderson PM, Hu FS and Brown TA (2009) Vegetation mediated the impacts of postglacial climate change on fire regimes in the south-central Brooks Range, Alaska. *Ecological Monographs* 79: 201–219.

Huerta MA, Whitlock C and Yale J (2009) Holocene vegetation–fire–climate linkages in northern Yellowstone National Park, USA. *Palaeogeography, Palaeoclimatology, Palaeoecology* 271: 170–181.

Jackson ST and Lyford ME (1999) Pollen dispersal models in Quaternary plant ecology: Assumptions, parameters, and prescriptions. *Botanical Review* 65: 39–75.

Knight DH (1991) The Yellowstone fire controversy. In: Keiter RB and Boyce MS (eds) *The Greater Yellowstone Ecosystem: Redefining America's Wilderness Heritage*. New Haven CT: Yale University Press, 87–104.

Larsen CPS and MacDonald GM (1998) Fire and vegetation dynamics in a jack pine and black spruce forest reconstructed using fossil pollen and charcoal. *Journal of Ecology* 86: 815–828.

Littell JS, McKenzie D, Peterson DL and Westerling AL (2009) Climate and wildfire area burned in western U. S. ecoprovinces, 1916–2003. *Ecological Applications* 19: 1003–1021.

Long CJ, Whitlock C, Bartlein PJ and Millspaugh SH (1998) A 9000-year fire history from the Oregon Coast Range, based on a high-resolution charcoal study. *Canadian Journal of Forest Research* 28: 774–787.

Lynch JA, Clark JS and Stocks BJ (2004) Charcoal production, dispersal and deposition from the Fort Providence experimental fire: Interpreting fire regimes from charcoal records in boreal forests. *Canadian Journal of Forest Research* 34: 1642–1656.

Marlon J, Bartlein PJ and Whitlock C (2006) Fire–fuel–climate linkages in the northwestern USA during the Holocene. *The Holocene* 16: 1059–1071.

Marlon JR, Bartlein PJ, Carcaillet C, Gavin DG, Harrison SP, Higuera PE *et al.* (2008) Climate and human influences on global biomass burning over the past two millennia. *Nature Geoscience* 1: 697–702.

Marlon JR, Bartlein PJ, Walsh MK, Harrison SP, Brown KJ, Edwards ME *et al.* (2009) Wildfire responses to abrupt climate change in North America. *Proceedings of the National Academy of Sciences of the United States of America* 106: 2519–2524.

Millspaugh SH and Whitlock C (1995) A 750-year fire history based on lake sediment records in central Yellowstone National Park, USA. *The Holocene* 5: 283–292.

Millspaugh SH, Whitlock C and Bartlein P (2000) Variations in fire frequency and climate over the past 17000 yr in central Yellowstone National Park. *Geology* 28: 211–214.

Neter J, Kuutner MH, Nachtsheim CJ and Wasserman W (1996) *Applied Linear Regression Models*. Boston: McGraw-Hill.

Peters ME and Higuera PE (2007) Quantifying the source area of macroscopic charcoal with a particle dispersal model. *Quaternary Research* 67: 304–310.

Pisaric MFJ (2002) Long-distance transport of terrestrial plant material by convection resulting from forest fires. *Journal of Paleolimnology* 28: 349–354.

Power MJ, Marlon J, Ortiz N *et al*. (2008) Changes in fire regimes since the Last Glacial Maximum: An assessment based on a global synthesis and analysis of charcoal data. *Climate Dynamics* 30: 887–907.

Renkin RA and Despain DG (1992) Fuel moisture, forest type, and lightning-caused fire in Yellowstone National Park. *Canadian Journal of Forest Research* 22: 37–45.

Romme WH (1982) Fire and landscape diversity in subalpine forests of Yellowstone National Park. *Ecological Monographs* 52: 199–221.

Romme WH and Despain DG (1989) Historical perspective on the Yellowstone fires of 1988. *Bioscience* 39: 695–699.

Schoennagel T, Veblen TT and Romme WH (2004) The interaction of fire, fuels, and climate across Rocky Mountain forests. *Bioscience* 54: 661–676.

Schoennagel T, Veblen TT, Romme WH, Sibold JS and Cook ER (2005) ENSO and PDO variability affect drought-induced fire occurrence in Rocky Mountain subalpine forests. *Ecological Applications* 15: 2000–2014.

Schrag AM, Bunn AG and Graumlich LJ (2008) Influence of bioclimatic variables on tree-line conifer distribution in the Greater Yellowstone Ecosystem: Implications for species of conservation concern. *Journal of Biogeography* 35: 698–710.

Sibold JS and Veblen TT (2006) Relationships of subalpine forest fires in the Colorado Front Range with interannual and multidecadal-scale climatic variation. *Journal of Biogeography* 33: 833–842.

Sugita S (1993) A model of pollen source area for an entire lake surface. *Quaternary Research* 39: 239–244.

Sugita S (2007) Theory of quantitative reconstruction of vegetation I: Pollen from large sites REVEALS regional vegetation composition. *The Holocene* 17: 229–241.

Tinker DB, Romme WH and Despain DG (2003) Historic range of variability in landscape structure in subalpine forests of the Greater Yellowstone Area, USA. *Landscape Ecology* 18: 427–439.

Tinner W, Conedera M, Ammann B, Gaggeler HW, Gedye S, Jones R *et al.* (1998) Pollen and charcoal in lake sediments compared with historically documented forest fires in southern Switzerland since AD 1920. *The Holocene* 8: 31–42.

Tinner W, Hofstetter S, Zeugin F, Conedera M, Wohlgemuth T, Zimmermann L *et al.* (2006) Long-distance transport of macroscopic charcoal by an intensive crown fire in the Swiss Alps – Implications for fire history reconstruction. *The Holocene* 16: 287–292.

Tinner W, Bigler C, Gedye S, Gregory-Eaves I, Jones RT, Kaltenrieder P *et al.* (2008) A 700-year paleoecological record of boreal ecosystem responses to climatic variation from Alaska. *Ecology* 89: 729–743.

Turner MG, Hargrove WW, Gardner RH and Romme WH (1994) Effects of fire on landscape heterogeneity in Yellowstone National Park, Wyoming. *Journal of Vegetation Science* 5: 731–742.

Welch PD (1967) The use of Fast Fourier Transforms for the estimation of power spectra: A method based on time averaging over short, modified periodograms. *IEEE Transactions of Audio and Electroacoustics* 15: 70–73.

Westerling AL, Hidalgo HG, Cayan DR and Swetnam TW (2006) Warming and earlier spring increase western US forest wildfire activity. *Science* 313: 940–943.

Whitlock C and Millspaugh SH (1996) Testing the assumptions of fire-history studies: An examination of modern charcoal accumulation in Yellowstone National Park, USA. *The Holocene* 6: 7–15.

Whitlock C, Bianchi MM, Bartlein PJ, Markgraf V, Marlon J, Walsh M *et al.* (2006) Postglacial vegetation, climate, and fire history along the east side of the Andes (lat 41–42.5 degrees S), Argentina. *Quaternary Research* 66: 187–201.

Whitlock C, Marlon J, Briles C, Brunelle A, Long C and Bartlein P (2008) Long-term relations among fire, fuel, and climate in the north-western US based on lake-sediment studies. *International Journal of Wildland Fire* 17: 72–83.

Woodhouse CA, Gray ST and Meko DM (2006) Updated streamflow reconstructions for the Upper Colorado River Basin. *Water Resources Research* 42: 1–16.